# Hot Electron Generation in Aqueous Solution at Oxide-Covered Tantalum Electrodes. Reduction of Methylpyridinium and Electrogenerated Chemiluminescence of $Ru(bpy)_3^{2+}$

**Frédéric Gaillard, Yung-Eun Sung, and Allen J. Bard***

*Department of Chemistry and Biochemistry, University of Texas at Austin, Austin, Texas 78712*

*Received: June 30, 1998; In Final Form: November 16, 1998*

We describe the injection of hot electrons into an aqueous solution by use of a $Ta/Ta_2O_5$ electrode. Evidence for this process was obtained by studying the chemically irreversible reduction of *N*-methylpyridinium ion ($NMP^+$, $E° = -1.37$ V vs SHE). The reduction of $NMP^+$ gives rise to a radical which undergoes rapid dimerization to produce a water-insoluble species, 1,1-tetrahydrobipyridine (TBP), that deposits on the electrode surface. The deposit was analyzed by AFM, XPS, IR-reflectance, and TOF/SIMS to provide evidence of TBP formation. We also investigated the electrochemical reduction of $Ru(bpy)_3^{2+}$ to confirm the generation of hot electrons on a $Ta/Ta_2O_5$ electrode in water. The electrochemical and spectroelectrochemical results present a well-defined reduction wave at high overpotential on $Ta/Ta_2O_5$ which is not observed on Pt or Au electrodes. Reduction of $Ru(bpy)_3^{3+}$ at a $Ta/Ta_2O_5$ electrode produces emission (electrogenerated chemiluminescence) and provides additional evidence of hot electron injection.

## Introduction

In a previous paper,[1] we described the injection of hot electrons into a MeCN solution by means of a $Ta/Ta_2O_5$ electrode. Hot electrons in solution ($e_h^s$) are defined as electrons with thermal energies ($kT_h$) greater than the thermal energy ($kT$) of the solution or as electrons with an energy far above the Fermi level in solution (which is usually defined by the solution species that establish the electrochemical potential of an electron in solution or the redox potential). This injection occurs when the negative bias applied to the Ta electrode is of a sufficient magnitude to cause the electrons to attain energies at, or above, the conduction band edge of the native oxide ($Ta_2O_5$) film on the Ta surface (Figure 1). The injection process was recognized by production of electrogenerated chemiluminescence (ECL) by direct injection to a solution of thianthrene radical cation in MeCN. A number of previous papers describing hot carrier injection from metals and semiconductors into solution, usually by irradiation to produce hot carriers in the metal or semiconductor, were discussed in an earlier publication.[1] The $Ta/Ta_2O_5$ electrode was selected in this study because of the large band gap separating the valence and conduction band in the oxide. Macagno and Schultze studied, for example, the dependence of the growth of thin oxide films on Ta electrodes over a potential range of 0−10 V and a pH range of 0−14.[2] They showed an energy diagram for the passivating film and reported that cathodic hydrogen evolution occurred with a large overpotential that depended on the pH of the solution. Clechet et al.[3] determined the band gap of the oxide to be 4 eV based on photocurrent experiments.

In this paper, we investigate the generation of hot electrons in aqueous solutions at potentials well above those where hydrogen evolution occurs on electrodes like Pt. The main purpose of this work is to show that hot electrons injected into a solution can be used for electrochemical reactions of the type that can only take place on high hydrogen overpotential materials, like mercury, in aqueous solutions. This is analogous to the approach used by Koval et al. who studied the photoelectrochemical reduction of a Cu(I) complex to copper metal by hot electrons at an irradiated semiconductor, p-InP, electrode ($e_h^{sc}$) in MeCN[4] and $e_h^{sc}$ reduction of dibromomethylbenzene in MeCN by means of a p-InP/Pt rotating ring/disk electrode.[5] His work followed the initial proposal by Nozik and co-workers[6] about the possibility of photogeneration of hot electrons in irradiated semiconductor electrodes (p-GaAs and p-InP) and their injection into solution. Note, however, that in the work described here, hot electrons in solution are generated electrochemically, without necessarily forming hot electrons in the oxide and without irradiation, from thermalized electrons in the metal.

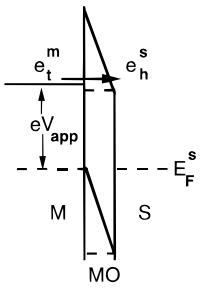


**Figure 1.** Schematic representation of electron injection across the oxide-covered metal electrode/liquid interface to produce hot electrons in solution phase.

In these studies, we used a well-known, irreversible, chemical reaction, the reduction of the *N*-methylpyridinium ion ($NMP^+$), to trap the hot electron produced with a $Ta/Ta_2O_5$ electrode. $NMP^+$ is reduced at −1.37 V vs SHE on a mercury electrode in water (1 M KCl) and cannot be reduced on Pt or Au electrodes because of the prior occurrence of hydrogen evolution.[7,8] The electrochemical reduction of $NMP^+$ in water occurs in a single electron-transfer reaction that produces the pyridinyl radical ($NMP^•$), which undergoes rapid dimerization ($k_f > 1 \times 10^7$ $M^{-1}$ $s^{-1}$) to produce a water-insoluble species which deposits on the electrode surface.

10.1021/jp982821k CCC: $18.00 
Published on Web 01/08/1999

$$NMP^+ + e \rightarrow NMP^\bullet \quad (1)$$

$$2NMP^\bullet \rightarrow TBP \text{ (precipitate)} \quad (2)$$

The occurrence of dimerization was established by Raghavan and Iwamoto[9] who treated the dimer, formed by electroreduction of 1-alkylpyridinium ion, with 1,4-benzoquinone. Their conclusions were based on the identification of the products by electrochemical and spectral techniques. Noorova and Volke[10] suggested that the dimerization is followed by further chemical reactions. In this study we focus our attention on the formation of the insoluble dimeric species and thus establish that the reduction of $NMP^+$ can be carried out on $Ta/Ta_2O_5$ by hot electrons.

We also investigated the electrochemical reduction of $Ru(bpy)_3^{2+}$ in 0.5 M KCl solution. It is well-established that the reduction of $Ru(bpy)_3^{2+}$ in nonaqueous solvents shows three characteristic reduction waves at −1.33, −1.52, and −1.76 V (vs SCE).[11] These potentials are not a strong function of the solvent, e.g., MeCN, dimethyl sulfoxide, dimethylformamide, or propylene carbonate. These waves correspond to simple, reversible, one-electron transfers to produce the +1, 0, and −1 species, representing successive reductions of the bpy ligands. The electrochemical reduction in water on a Pt electrode is not observed, because these waves lie well beyond hydrogen evolution. $Ru(bpy)_3^{2+}$ was reduced by electrons generated by pulse radiolysis in the presence of butyl alcohol,[12] where an absorption band at 510 nm ($\epsilon \approx 12000\ M^{-1}\ cm^{-1}$), attributed to the formation of the transient species $Ru(bpy)_3^{+}$, was detected. Its decay, by second-order kinetics, was explained by the disproportionation reaction

$$2Ru(bpy)_3^{+} + 2H^+ \xrightarrow{k} Ru(bpy)_3^{2+} + Ru(bpy)_2(bpyH_2)^{2+} \quad (3)$$

where $k$ is equal to $3.5 \times 10^8\ M^{-1}\ s^{-1}$.[11,12] The UV−vis spectrum of the dihydro-2,2′-bipyridine is very close to that of $Ru(bpy)_3^{2+}$ with an absorption band maximum at 450 nm. Moreover, it is well-known that $Ru(bpy)_3^{+}$ is a strong reducing agent and reacts with $O_2$[13] ($k$ of $10^8$−$10^9\ M^{-1}\ cm^{-1}$) and more slowly with protons and water. Henry and Hoffman[14] also reported hydrate formation of 2,2′-bipyridine and described the effect of base on the emission and absorption bands of bpy. This observation was used by Mullazani et al.[15] who suggested that the decay of $Ru(bpy)_3^{+}$ occurs through the intermediacy of a covalent hydrate species. Here we studied the generation of $Ru(bpy)_3^{+}$ in an aqueous solution at $Ta/Ta_2O_5$ and have used the ECL that occurs on reaction with $Ru(bpy)_3^{3+}$ to confirm that this species is formed. Numerous previous studies have shown that the excited state, $Ru(bpy)_3^{2+}*$, can be produced by the annihilation reaction between $Ru(bpy)_3^{3+}$ and $Ru(bpy)_3^{+}$ on a Pt electrode in nonaqueous solvents according to the following scheme[11,16,17]

$$Ru(bpy)_3^{2+} + e^- \rightarrow Ru(bpy)_3^{+} \quad (4)$$

$$Ru(bpy)_3^{2+} - e^- \rightarrow Ru(bpy)_3^{3+} \quad (5)$$

$$Ru(bpy)_3^{+} + Ru(bpy)_3^{3+} \rightarrow Ru(bpy)_3^{2+}* + Ru(bpy)_3^{2+} \quad (6)$$

$$Ru(bpy)_3^{2+}* \rightarrow Ru(bpy)_3^{2+} + h\nu \quad (7)$$

which produces a bright ECL signal at 625 nm (orange light). This experiment involves generation of excited states via homogeneous electron transfer between the electrogenerated oxidized ($Ru(bpy)_3^{3+}$) and reduced ($Ru(bpy)_3^{+}$) forms at the electrode by alternate application of potentials to cause oxidation and reduction of the complex. This annihilation reaction does not occur in aqueous solutions at either Pt (where $Ru(bpy)_3^{2+}$ is not reducible because of the hydrogen evolution) or Ta (where $Ru(bpy)_3^{2+}$ is not oxidizable) electrodes. Nevertheless, ECL emission of $Ru(bpy)_3^{2+}$ can be obtained by the use of a coreactant that generates a strong oxidant on reduction.[18] Thus, in the presence of persulfate ($S_2O_8^{2-}$), the mechanism proceeds as follows:

$$Ru(bpy)_3^{2+} + e^- \rightarrow Ru(bpy)_3^{+} \quad (8)$$

$$Ru(bpy)_3^{+} + S_2O_8^{2-} \rightarrow Ru(bpy)_3^{2+} + SO_4^{2-} + SO_4^{-} \quad (9)$$

The excited species is then produced by the oxidation of $Ru(bpy)_3^{+}$ by $SO_4^-$:

$$SO_4^{-} + Ru(bpy)_3^{+} \rightarrow Ru(bpy)_3^{2+}* + SO_4^{2-} \quad (10)$$

$$Ru(bpy)_3^{2+}* \rightarrow Ru(bpy)_3^{2+} + h\nu \quad (11)$$

These experiments were carried out in water−MeCN (1:1) mixtures to minimize hydrogen evolution and showed a relative ECL intensity that was a function of $S_2O_8^{2-}$ concentration (for 1 mM $Ru(bpy)_3^{2+}$, the intensity was highest at 15−20 mM $S_2O_8^{2-}$). Gleria and Memming[19] showed that $Ru(bpy)_3^{2+}*$ may also be formed by direct heterogeneous electron transfer at n-type SiC and n-GaP semiconductor electrodes in water and MeCN upon reduction of $Ru(bpy)_3^{3+}$. The electrochemical, spectroelectrochemical, and ECL experiments discussed below demonstrate that the reduction of $Ru(bpy)_3^{2+}$ and $Ru(bpy)_3^{3+}$ (with generation of ECL) can be performed at a $Ta/Ta_2O_5$ electrode in purely aqueous solutions via hot electrons.

## Experimental Section

**Reduction of *N*-Methylpyridinium Ion.** The *N*-methylpyridinium salt ($NMP-PF_6$) was prepared by metathesis of the iodide salt (NMPI), which was synthesized by a conventional procedure.[20] Ion exchange of NMPI was performed with potassium hexafluorophosphate (Aldrich, 98%). The precipitate of $NMP^+PF_6^-$ was filtered and recrystallized twice before drying overnight in a vacuum oven. Potassium chloride (EM Science) was used as the supporting electrolyte in Millipore water (Milli-Q system, 18 Ω-cm). The solution was bubbled for 15 min with Ar before each experiment.

The electrochemical cell was a conventional three-electrode cell. The working electrode was a square piece of $Ta/Ta_2O_5$ spot-welded to a Ta wire to provide the electrical contact and was polished before each experiment to give a bright reflective surface. The reference and auxiliary electrodes were Ag/AgCl and Pt grid electrodes, respectively.

The cyclic voltammetry experiments were carried out with a model 660 electrochemical workstation (CH Instruments, Memphis, TN). Bulk electrolyses were performed with the same equipment at a fixed potential (−1.6 V vs Ag/AgCl) for durations of 3−30 min. The $Ta/Ta_2O_5$ was then removed and dried with argon. Any deposit observed on the electrode was examined by atomic force microscopy (AFM), X-ray photoelectron spectroscopy (XPS), IR-reflectance, and secondary-ion mass spectrometry (TOF/SIMS) at room temperature. The AFM was a Nanoscope III (Digital Instruments, Santa Barbara, CA). The XPS experiments were performed with the PHI 5700 ESCA system (Physical Electronics Equipment) (Al Kα anode, 1487.7 eV). The sample was placed in a UHV chamber which was

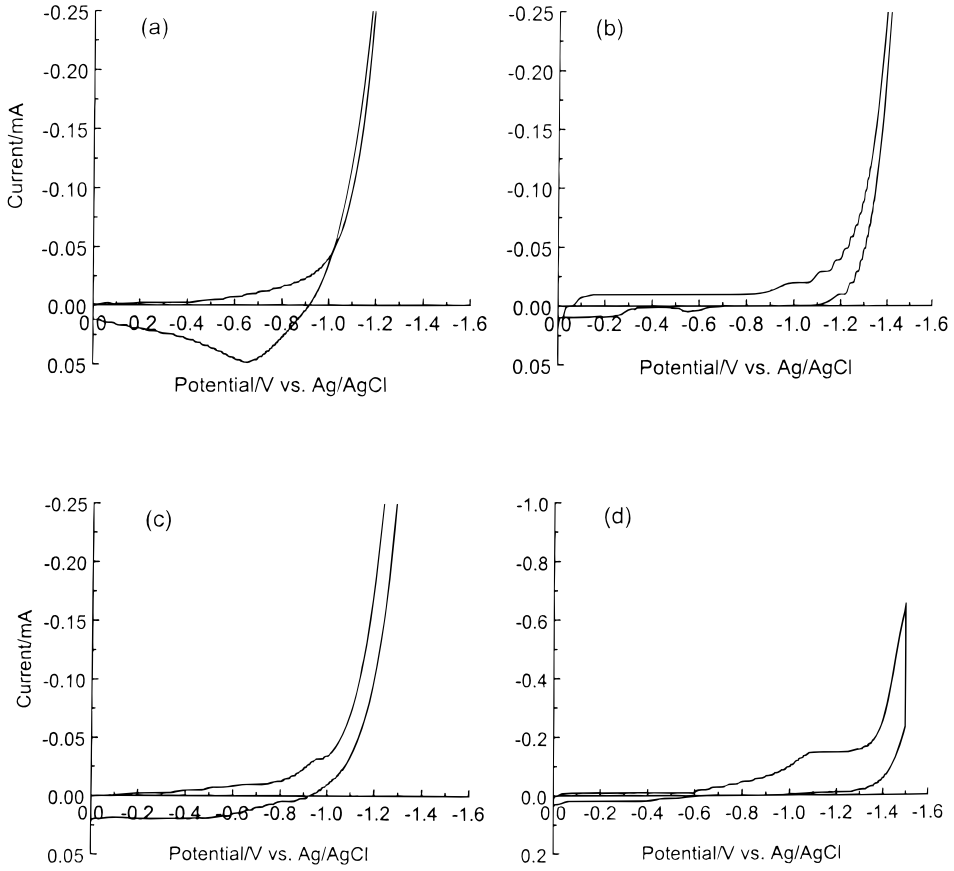


**Figure 2.** Cyclic voltammograms at 100 mV/s: (a) Pt and (b) $Ta/Ta_2O_5$ in aq 0.5 M KCl and (c) Pt and (d) $Ta/Ta_2O_5$ in aq 10 mM *N*-methylpyridinium, 0.5 M KCl.

pumped down to low $10^{-10}$ Torr. The IR-reflectance experiments utilized an FT-IR spectrometer from Nicolet (model 550 Magma). The IR-beam was reflected from the electrode with an incidence angle of 85° and then analyzed by an MCT detector. Each spectrum was obtained over the range 1000−4000 $cm^{-1}$ with a resolution of 4 $cm^{-1}$. The background spectrum was recorded with the same electrode used as the working electrode during the electrolysis. The Kramers−Kronig transform was not applied to correct for possible variations in the refractive index of the film. The TOF/SIMS experiments were performed with a time-of-flight secondary ion mass spectrometer from Physical Electronics Equipment ($Cs^+$, 8 keV).

**Reduction of $Ru(bpy)_3^{2+}$. Electrochemistry.** Tris(2,2′-bipyridyl)ruthenium(II) chloride hexahydrate (98%, Strem Chemicals) and KCl (EM Science), the supporting electrolyte, were used as received and dissolved in fresh Millipore water. The solution was then deaerated for 15 min. Voltammetric experiments were performed in the same electrochemical system as that previously described for the experiments in MeCN.[1] Spectroelectrochemical experiments were carried out to observe variations in the absorption spectra during a potential scan. The spectra were acquired in the range 350−750 nm with a Spectronic 3000 spectrometer (Milton Roy) equipped with a photodiode array. The voltammograms were recorded with a BAS 100 electrochemical analyzer (Bioanalytical Systems). A spectroelectrochemical cell was specially designed to perform these experiments. The working electrode was a $Ta/Ta_2O_5$ spiral wire which was sandwiched between pieces of glass and ITO (indium tin oxide). The ITO surface was scratched to produce three electrically isolated parts, one that was used as the working electrode and two that were used for the auxiliary and reference electrodes and hidden from the UV−vis beam with black adhesive tape. In this way, species generated at the counter electrode during the electrochemical reactions were not included in the spectrophotometric experiments. The light beam was guided perpendicularly to the surface defined by the working electrode with a path length typically below 1 mm.

**ECL Experiments.** Electrochemical measurements were carried out with a model 175 universal programmer and a model 173 potentiostat (Princeton Applied Research, Princeton, NJ) with an Omnigraphic 2000 *x*−*y* recorder (Houston Instruments, Austin, TX). The ECL emission was imaged with a CCD camera (model CH210, Photometrics Ltd., Tucson, AZ) cooled to −125 °C. The ECL emission-potential transient was measured with a model C1230 single-photon counting system (Hamamatsu Corp., Bridgewater, NJ) utilizing a Hamamatsu R928P photomultiplier tube cooled to −20 °C in a model TE308 TSRF cooler controller (Products for Research Inc., Danvers, MA). The meter output was fed into the *y*-axis of the *x*−*y* recorder, and the signal from the potentiostat was fed into the *x*-axis to afford ECL intensity vs bias displays.

## Results and Discussion

**Reduction of *N*-Methylpyridinium Ion.** Figures 2a and 2b show voltammograms of a 0.5 M KCl solution on Pt and $Ta/Ta_2O_5$ electrodes, respectively. On the Pt electrode, no current is observed before hydrogen evolution at −1.2 V vs Ag/AgCl. However, as expected from previous experiments in MeCN,[1] the potential for proton or water reduction in aqueous solutions is shifted to −1.5 V vs Ag/AgCl on a $Ta/Ta_2O_5$ electrode. On both electrodes, as soon as the current increased, bubbles indicating hydrogen evolution were observed. The location of the Fermi level of the oxide was determined from current−

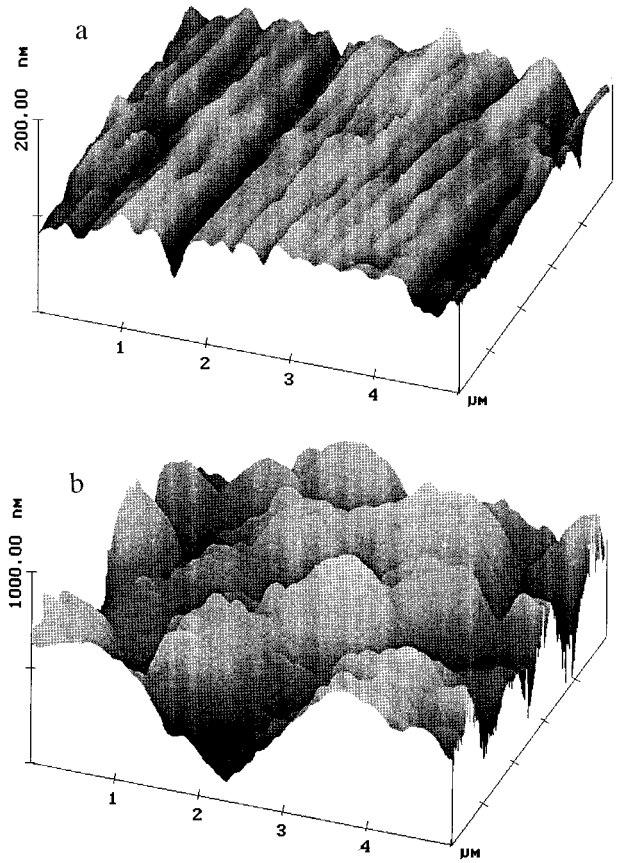


**Figure 3.** AFM image of the $Ta/Ta_2O_5$ electrode (a) before electrolysis and (b) after electrolysis in 10 mM *N*-methylpyridinium solution at −1.6 V vs Ag/AgCl for 3 min.

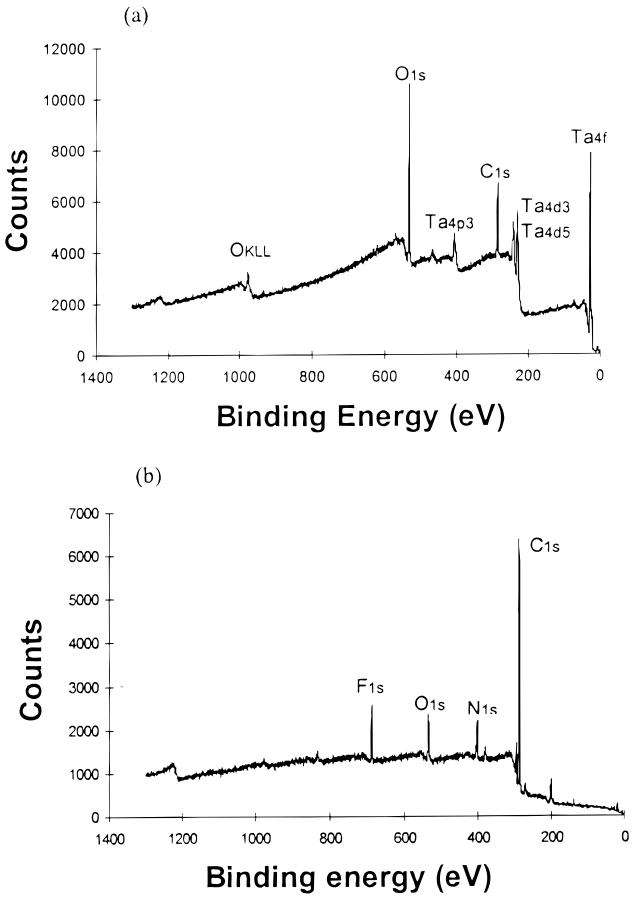


**Figure 4.** XPS results for the $Ta/Ta_2O_5$ electrode (a) before electrolysis and (b) after electrolysis in 10 mM *N*-methylpyridinium solution at −1.6 V vs Ag/AgCl for 3 min.

potential curves for $Ta/Ta_2O_5$ in a 0.5 M KCl solution under illumination with a Xe lamp. Upon irradiation of the electrode an anodic photocurrent appears. The flatband potential can be estimated from the onset potential of the photocurrent, which is at −1.1 V vs SCE. This result is similar to the published data for an aqueous system at pH 7.[1] No significant current appears at a potential lower than −1.5 V. This observation is consistent with the fact that electron transfer occurs via the $Ta_2O_5$ conduction band and not via direct tunneling through the oxide. Consequently, the electrons that are generated from the $Ta/Ta_2O_5$ electrode can be considered as hot solution-phase electrons as previously found in MeCN.[1]

Similar results were obtained with a solution of *N*-methylpyridinium ($NMP^+$) (10 mM) in aq KCl (0.5 M) (Figure 2c, d). On a Pt electrode, no reduction of $NMP^+$ is observed before the hydrogen evolution at −1.2 V (vs Ag/AgCl). However, on a $Ta/Ta_2O_5$ electrode, a small current, attributed to $NMP^+$ reduction, appears at −1.0 V and remains constant until −1.4 V, where hydrogen evolution begins. To confirm the electrochemical reduction of $NMP^+$ on $Ta/Ta_2O_5$, as indicated on the voltammogram, we performed bulk electrolysis of the solution at −1.6 V and analyzed ex situ the deposit by different techniques as shown below.

**AFM Experiments**. AFM was used to compare the surface morphology of the Ta electrode before and after the electrochemical experiments. An image of the $Ta/Ta_2O_5$ electrode obtained before bulk electrolysis (Figure 3a) shows a rough surface with regular parallel lines, probably generated during mechanical polishing of the electrode. The depth of these grooves never exceeded 100 nm. An image of the same electrode after a bulk electrolysis at −1.6 V (vs Ag/AgCl) for 3 min (Figure 3b) shows a strong difference of morphology compared to that in Figure 3a. The surface is now composed of spherical aggregates which cover the grooves observed initially on $Ta/Ta_2O_5$ and the roughness is larger. This shows the formation of a deposit on the electrode and is evidence of the electrochemical reduction of *N*-methylpyridinium in water on the Ta electrode. This deposit can be attributed to the formation of the 1,1-dimethyltetrahydrobipyridine (TBP) species, as demonstrated below.

**XPS Experiments.** Figure 4a shows the XPS results of the $Ta/Ta_2O_5$ electrode before electrolysis. The spectrum is mainly composed of seven peaks situated at 27, 230, 240, 285, 405, 531, and 976 eV. Three of these ($Ta_{4p3/2}$ at 405 eV, $Ta_{4d3/2}$ at 240 eV, and $Ta_{4p5/2}$ at 230 eV) are characteristic of the presence of elemental Ta. The intense $O_{1s}$ line at 531 eV, accompanied by the $O_{KLL}$ Auger line at 976 eV, characterizes the presence of oxygen. These Ta and oxygen contributions are attributed to the oxide layer of $Ta_2O_5$ on the electrode, although oxygen can also indicate some contamination by air before the XPS experiment. This last observation is supported by the existence of a weak $C_{1s}$ line at 285 eV, which shows the presence of carbon on the electrode. Figure 4b shows the results of an XPS experiment carried out on the $Ta/Ta_2O_5$ electrode after a bulk electrolysis in $NMP^+$ at −1.6 V for 3 min. The spectrum obtained for electrolysis for 30 min showed similar characteristics. The first experimental evidence of film formation is the absence of the Ta peaks in the spectrum, indicating that the electrode surface is effectively covered by a film and that no photoelectron is sufficiently energetic to be emitted from the oxide layer through the film. Nevertheless, the oxygen line ($O_{1s}$

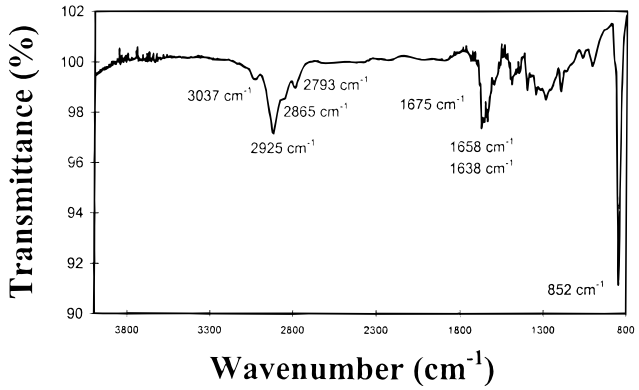


**Figure 5.** IR-reflectance spectrum of the $Ta/Ta_2O_5$ after electrolysis in 10 mM *N*-methylpyridinium solution at −1.6 V vs Ag/AgCl for 3 min. The resolution is 4 $cm^{-1}$.

at 531 eV) is still observed and is probably due to contamination of the electrode by air. On the other hand, a predominant line at 285 eV and another one at 400 eV characterize the presence of carbon ($C_{1s}$ line) and nitrogen ($N_{1s}$ line) on the electrode. Here, the relative intensity of the carbon ($C_{1s}$) is higher than the oxygen ($O_{1s}$) before the electrochemical experiment. Thus, even if the presence of oxygen suggests that the electrode was contaminated before the XPS analysis, such an amount of carbon cannot be provided only from this source (compare to Figure 4a) and the observation of nitrogen ($N_{1s}$ at 400 eV) confirms that a film containing C and N is deposited on the electrode. The ratio of the area defined by the $C_{1s}$ and $N_{1s}$ line gives 9.9 and 7.1 for the different electrodes (electrolysis for 3 and 30 min, respectively). This ratio does not take into account the presence of carbon due to other sources, which can explain the difference of these values with the value theoretically expected of 6 for formation of TBP. Finally, a peak at around 687 eV assigned to elemental fluorine is also observed in the spectrum. Its presence suggests that some $PF_6^-$ ion used during the metathesis of the iodide salt was not totally removed after drying the electrode with Ar and is entrapped in the film.

**IR-Reflectance Experiments.** The IR-reflectance experiments were carried out to detect vibrations that can be attributed to TBP deposited on the surface. The dimerization is not the only step that can occur in the reduction of $NMP^+$,[9,10] but the objective of this work was not to characterize all of the peaks of the spectrum but rather to show that $NMP^+$ can be reduced on $Ta/Ta_2O_5$ in water. Figure 5 is an IR spectrum of the electrode obtained after electrolysis of the solution (10 mM $NMP^+$, 0.5 M KCl) at −1.6 V for 3 min. The transmittance spectrum of the bare electrode was used as a reference, so all peaks observed are effectively background subtracted. Three absorption regions are observed: a region composed of four peaks situated at 2780, 2820, 2925, and 3050 $cm^{-1}$; the fingerprint region between 1000 and 1600 $cm^{-1}$; and a strong absorption peak at about 850 $cm^{-1}$. Vibration peaks in the 2750−3100 $cm^{-1}$ range can be attributed to the C−H, $CH_3$ stretching vibrations, to the C−H stretching vibrations in the N−C−H bond (2820 $cm^{-1}$), or to functional groups such as N−$CH_3$ (2780 $cm^{-1}$). In the fingerprint region, the strong absorption peaks in the 1600−1650 $cm^{-1}$ range can be assigned to isolated C═C double bonds. This region also exhibits numerous unidentified peaks of medium intensity between 1000 and 1500 $cm^{-1}$. No absorption vibrations attributed to O−H (in the 3550−3650 $cm^{-1}$ range for the stretching vibration) or C═O vibrations (in the 1700−1750 $cm^{-1}$ range) were observed. Despite the complexity of the IR spectrum, this experiment

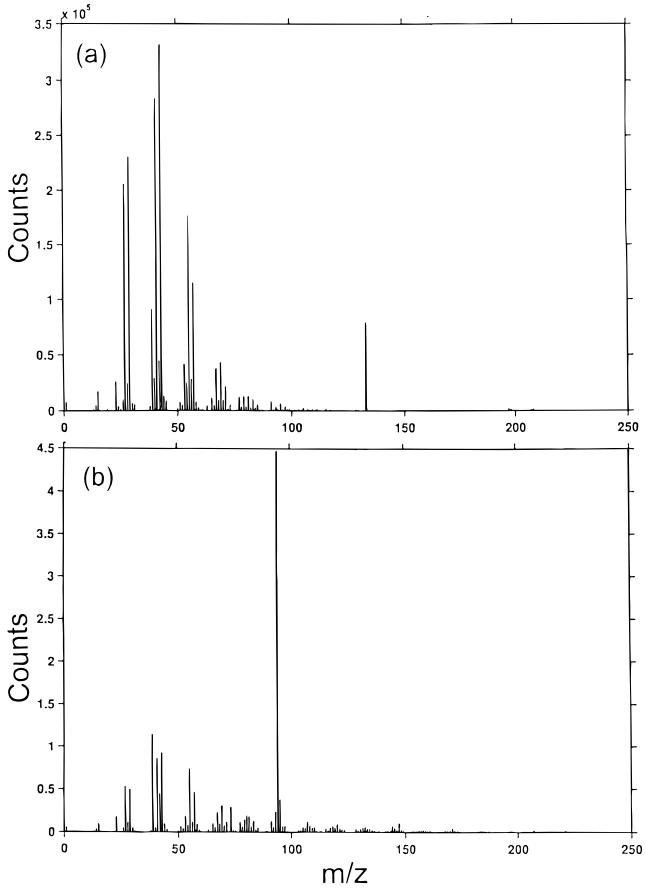


**Figure 6.** TOF/SIMS spectrum in the range of $m/z = 90-100$ for the $Ta/Ta_2O_5$ electrode (a) before the electrochemical experiment and (b) after the electrolysis in 10 mM *N*-methylpyridinium solution at −1.6 V vs Ag/AgCl for 3 min.

confirms the deposition observed by AFM and XPS on the electrode and shows that the film possesses organic functionalities consistent with the dimer structure. Finally, we assign the band at 850 $cm^{-1}$ to the vibration of the P−F bond, which shows an infrared band in this region.[21] This result is consistent with the XPS results and the observation of the fluorine in the spectrum.

**TOF/SIMS Experiments.** TOF/SIMS spectra of the $Ta/Ta_2O_5$ electrodes before and after electrochemical experiments exhibit numerous peaks which are mainly due to organic species. Some of the peaks observed with the reference $Ta/Ta_2O_5$ electrode must be attributed to surface carbonaceous contamination. Here, we focus on the range of $m/z = 90-100$. No significant peaks are observed in this region for the $Ta/Ta_2O_5$ electrode (Figure 6a), but for the electrode used during bulk electrolysis, an intense peak at 94.0638 is found (Figure 6b). This peak can be assigned to the $C_6H_8N$ fragment, molecular weight 94.0657 g/mol, equal to one-half of the expected dimeric species ($M = 188.131$ g/mol). This result is simply interpreted in terms of $C_4-C_{4'}$ bond cleavage to release the stable fragment $C_6H_8N$ and confirms the probable formation of TBP on the $Ta/Ta_2O_5$ electrode.

A similar experiment was performed on a Pt electrode where a potential of −1.6 V vs Ag/AgCl was applied for 3 min. No evidence of deposition was observed under the same conditions. During the potential step, a large amount of hydrogen evolution was observed on Pt, contrary to the results with the Ta electrode.

**Reduction of Tris(2,2′-bipyridyl)ruthenium. Electrochemical Experiments.** Voltammograms of a 0.5 M KCl aqueous solution with and without 1 mM $Ru(bpy)_3^{2+}$ are shown in

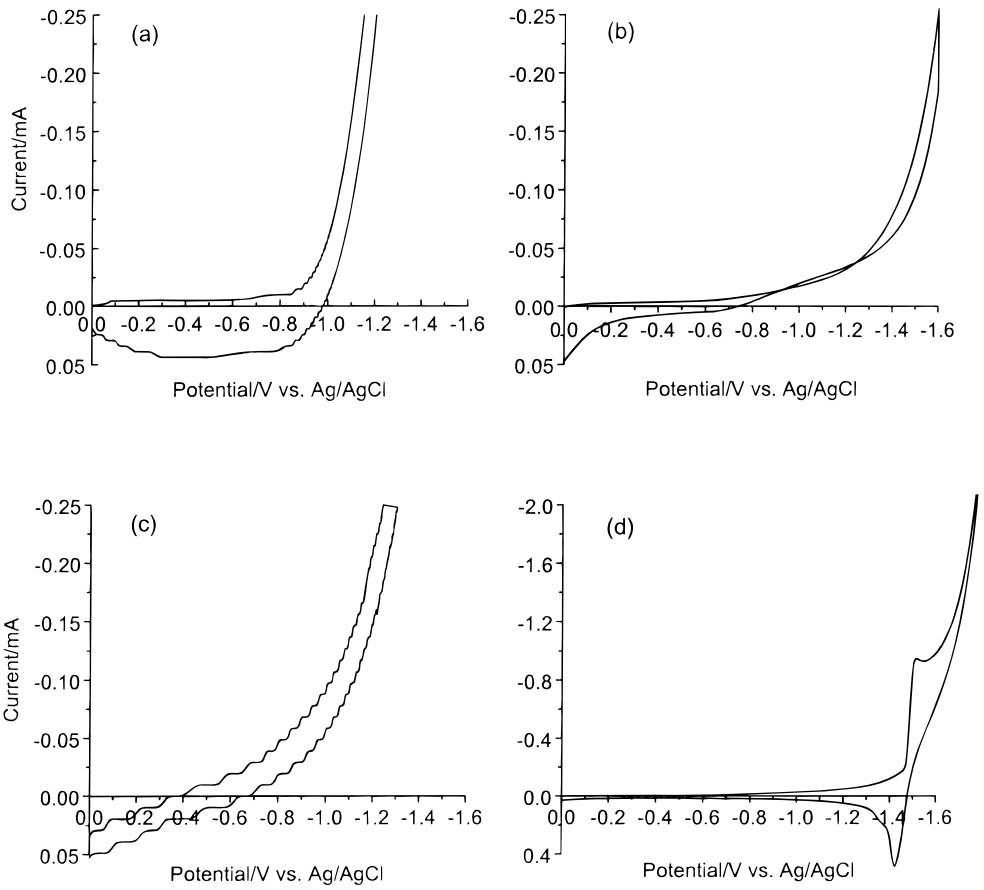


**Figure 7.** Cyclic voltammograms at 100 mV/s at (a) Pt and (b) $Ta/Ta_2O_5$ in aq 0.5 M KCl and (c) Pt and (d) $Ta/Ta_2O_5$ in aq 1 mM $Ru(bpy)_3^{2+}$, 0.5 M KCl.

Figure 7 on Pt and $Ta/Ta_2O_5$ electrodes. On Pt (Figure 7a,c), as expected, the reduction wave of $Ru(bpy)_3^{2+}$ is not observed. However, on Ta (Figure 7b,d), the current increases strongly at a potential of −1.5 V and a reduction wave is observed just before hydrogen evolution. Complementary experiments were carried out to prove that the wave can be attributed to the reduction of $Ru(bpy)_3^{2+}$. First, when increased amounts of $Ru(bpy)_3^{2+}$were added to the solution, the intensity of the wave increased (not shown). We also performed spectroelectrochemical experiments to characterize the formation of $Ru(bpy)_3^{+}$ from its absorption spectrum. Figure 8 presents the results obtained for a spectroelectrochemical experiment at a scan rate of 20 mV/s. Each spectrum was recorded in 8 s (160 mV), and two consecutive spectra were obtained every 10 s (every 200 mV). Because the solution is colored (absorption band of $Ru(bpy)_3^{2+}$ at 450 nm), the reference spectrum used for the calculation of the absorbance was taken as the initial solution. Thus, when no current was observed at the electrode, the corrected absorbance was zero at all wavelengths. When a current appeared (at −1.75 V vs ITO), the absorbance at 450 nm decreased (Figure 8c) but no absorption band (at 510 nm) which can be attributed to the formation of $Ru(bpy)_3^{+}$ was observed. This observation is consistent with the known instability of $Ru(bpy)_3^{+}$ in aqueous systems; the short lifetime found in pulse radiolysis experiments[12] suggests that it would not be observed in the spectroelectrochemical experiments at slow scan rates. For the same experiment carried out at higher scan rates (50 and 100 mV/s), the same results were obtained; i.e., the absorbance at $A_{450\ nm}$ decreased when the potential scan encompassed the reduction wave (not shown). While $Ru(bpy)_3^{+}$ is never observed during these experiments, probably because the lifetime of the species is not sufficiently long, the decrease at 450 nm can only be attributed to the reduction of $Ru(bpy)_3^{2+}$. Because the counter electrode was well outside the path of the light beam, processes that occur there, e.g., oxidation of $Ru(bpy)_3^{2+}$, do not affect the spectrophotometric response. Moreover, the decrease at 450 nm can also not be attributed to the formation of bubbles in the light path because of proton reduction. On the reverse scan, after the scan on the reduction wave, an unusual, sharp, peak was observed in the voltammogram. The peak height of this wave decreased at higher pH. A similar experiment was carried out in aq 0.5 M KCl with a mercury electrode (Figure 9), and the same results were observed. This sharp peak can probably be attributed to precipitation or strong adsorption of the uncharged complex on $Ta/Ta_2O_5$ electrode, because the wave occurs at potentials corresponding to reduction of $Ru(bpy)_3^{2+}$ to the $Ru(bpy)_3^{+}$ and $Ru(bpy)_3^{0}$ species in pure MeCN. All these results support the idea that the wave observed on $Ta/Ta_2O_5$ must be attributed to the reduction of $Ru(bpy)_3^{2+}$.

**ECL Experiments.** To confirm that $Ru(bpy)_3^{+}$ is effectively generated during the electrochemical reduction of $Ru(bpy)_3^{2+}$ in water on $Ta/Ta_2O_5$, ECL experiments were carried out. A solution containing the oxidized precursor ($Ru(bpy)_3^{3+}$) was prepared by addition of an excess of $PbO_2$ in 0.1 M $HClO_4$ solution. Figure 10a shows the ECL spectrum produced at a $Ta/Ta_2O_5$ electrode in this solution. The $Ta/Ta_2O_5$ electrode produced an ECL signal at potentials below −1.6 V (Figure 10b). This can be attributed to the $Ru(bpy)_3^{3+}/Ru(bpy)_3^{+}$ annihilation mechanism[11,16,17] and signals $Ru(bpy)_3^{+}$ formation at the Ta electrode. Alternatively, the excited state could be produced by electron transfer from the electrode directly into

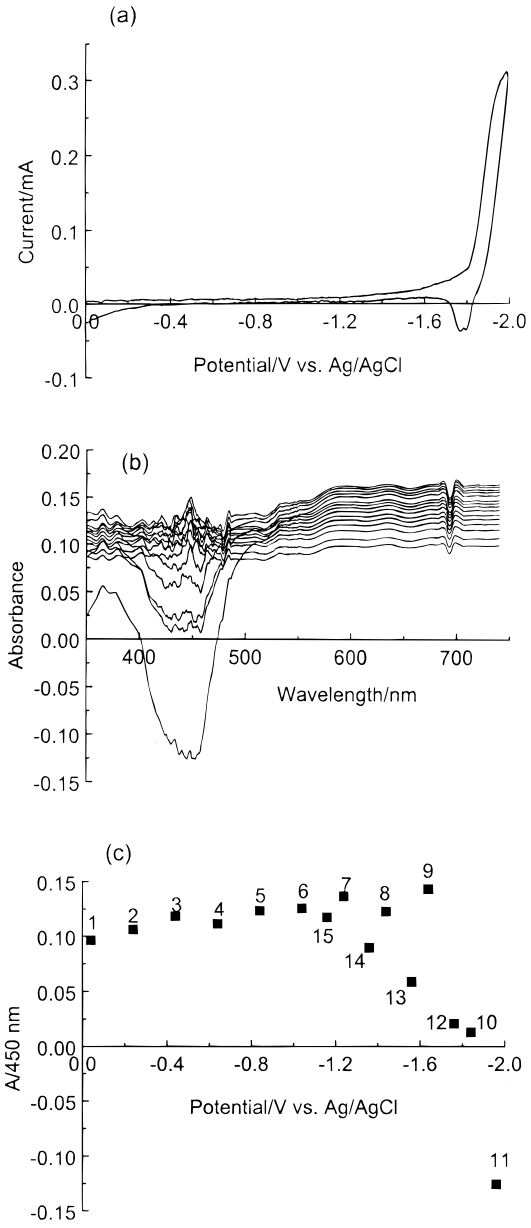


**Figure 8.** (a) Voltammogram of an aq 1 mM $Ru(bpy)_3^{2+}$, 0.5 M KCl solution; scan rate, 20 mV/s. (b) Absorption spectra recorded during the voltammetry experiment. (c) Variation of $A_{450\ nm}$ with time; 15 spectra, 10 s cycle time, 10 s acquisition time.

an upper (bpy) orbital of $Ru(bpy)_3^{3+}$ (a hot electron mechanism):

$$Ru(bpy)_3^{3+} + e^- \rightarrow Ru(bpy)_3^{2+}* \quad (12)$$

$$Ru(bpy)_3^{2+}* \rightarrow Ru(bpy)_3^{2+} + h\nu \quad (13)$$

In either case, the results show that production of ECL from $Ru(bpy)_3^{3+}$ in an aqueous solution without addition of a coreactant at a $Ta/Ta_2O_5$ electrode is possible. This ECL was stable on the Ta electrode for several hours (Figure 10c). Note that hydrogen evolution and the reduction of $Ru(bpy)_3^{3+}$ occur on $Ta/Ta_2O_5$ at about the same potential, so that hydrogen evolution occurs during the reduction of $Ru(bpy)_3^{3+}$.

Additional evidence for the reduction of $Ru(bpy)_3^{2+}$ in water is based on the use of $S_2O_8^{2-}$ as a coreactant. A solution of 1 mM $Ru(bpy)_3^{2+}$, 20 mM $S_2O_8^{2-}$, and 0.5 M KCl in water was studied because, under these conditions, the ECL signal was around its maximum value. The voltammogram of this solution

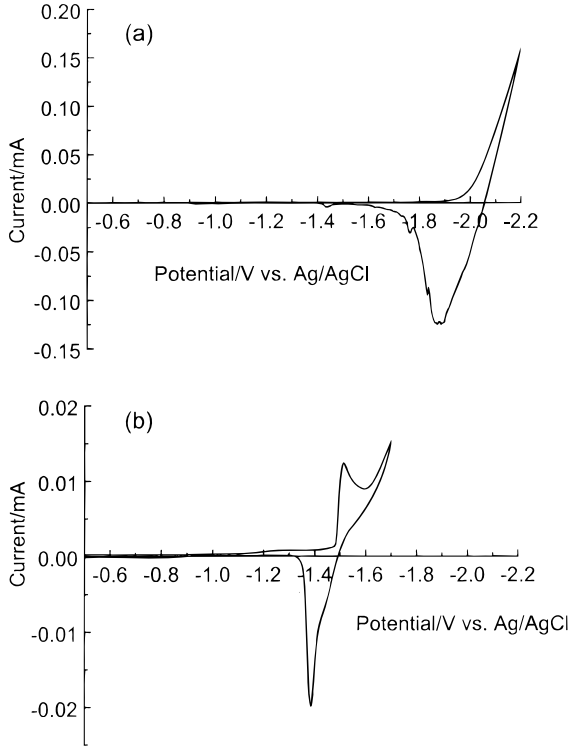


**Figure 9.** Cyclic voltammograms at a Hg electrode at 100 mV/s (a) aq 0.5M KCl and (b) aq 1 mM $Ru(bpy)_3^{2+}$, 0.5 M KCl.

at $Ta/Ta_2O_5$ shows two successive waves. The first one characterizes the reduction of $S_2O_8^{2-}$ according to the mechanism:

$$S_2O_8^{2-} + e^- \rightarrow S_2O_8^{3-} \quad (14)$$

$$S_2O_8^{3-} \rightarrow SO_4^{2-} + SO_4^- \quad (15)$$

The second one corresponds to the reduction of $Ru(bpy)_3^{2+}$. A potential step to −1.6 V vs Ag/AgCl produces ECL. The spectrum showed the well-known peak at 625 nm, which is characteristic of the orange luminescence of the $Ru(bpy)_3^{2+}*$ (Figure 11). Moreover, a correlation between the electrode potential and the ECL emission, shown in Figure 11, indicates that ECL appears during the reduction of $Ru(bpy)_3^{2+}$, so that the ECL can be explained by the sequence of reactions in eqs 10 and 11, which take account of the electrochemical formation of $Ru(bpy)_3^+$ during the potential step.

## Conclusion

In this paper, we have demonstrated the generation of solution-phase hot electrons at an oxide-covered metal electrode in aqueous solutions. The reduction of the *N*-methylpyridinium ion to produce a film on the electrode surface was shown. The nature of this organic film was studied by AFM, XPS, IR-reflectance, and TOF/SIMS and was consistent with the mechanism proposed for experiments performed with a mercury electrode,[7−10] where the film is taken as 1,1-dimethyltetrahydrobipyridine. These results show that the *N*-methylpyridinium ion can be reduced on $Ta/Ta_2O_5$ in aq KCl at a potential where hydrogen evolution prevents its reduction on Au or Pt. $Ru(bpy)_3^{2+}$ can also be reduced at a Ta electrode in aqueous solution, although the mechanism is more complex in water than in a nonaqueous solvent. These studies suggest the possible use of oxidized metal electrodes to perform electrochemical reactions that were only possible on a high hydrogen overpotential

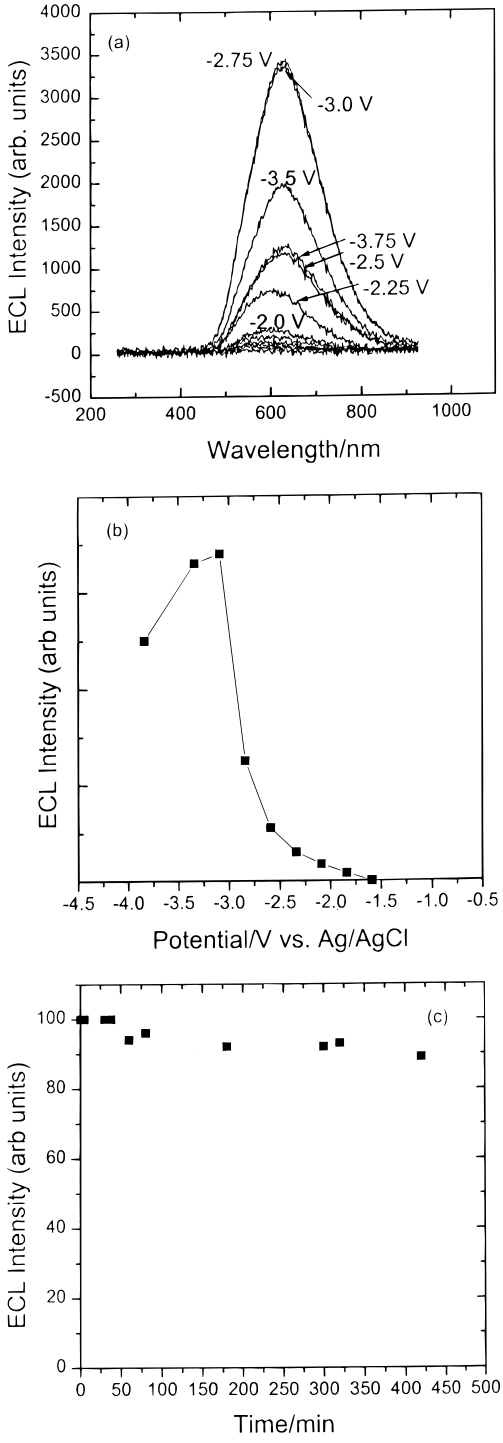


**Figure 10.** ECL of solutions of 0.5 mM $Ru(bpy)_3^{3+}$, 0.1 M $HClO_4$ with excess $PbO_2$. (a) ECL spectra at a Ta electrode; exposure time, 30 s. (b) ECL intensity as a function of the cathodic pulse potential; 0.1 s cycling between 0 V and the negative potentials shown. (c) ECL intensity as a function of the time; 0.1 s cycling between 0 V and −2.75 V.

metal like mercury. ECL at the $Ta/Ta_2O_5$ electrode may also be of interest in analytical applications where light generation in the absence of a coreactant in aqueous media should be possible. The use of other insulating films with large band gaps, e.g., $SiO_2$, to extend the range of potential is of interest.

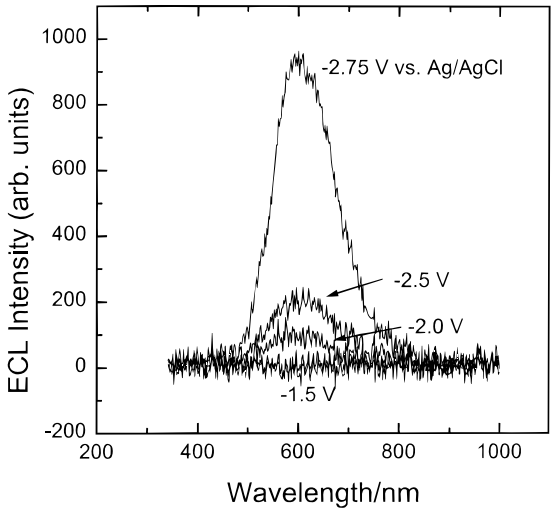


**Figure 11.** ECL spectra for different $Ta/Ta_2O_5$ electrodes in 1 mM $Ru(bpy)_3^{2+}$, 20 mM $S_2O_8^{2-}$, 0.5 M KCl; 30 s exposure. The potential was stepped between 0 and −1.60 V vs Ag/AgCl.

**Acknowledgment.** The support of this research by the National Science Foundation (CHE-9423874) and the Robert A. Welch Foundation is gratefully acknowledged. We thank Dr. Peter M. Blass and Dr. Eddie Pylant for the XPS and TOF/SIMS measurements and Kai Hu for AFM experiments. We also thank Dr. Radha Pyati for helpful discussions concerning this work.

## References and Notes

(1) Sung Y.-E.; Gaillard F.; Bard A. J. *J. Phys. Chem. B* **1998**, *102*, 9797.
(2) Macagno, V.; Schultze, J. W. *J. Electroanal. Chem.* **1984**, *180*, 157.
(3) Clechet, P.; Martin, J. R.; Olier, R.; Vallouy, C. *C. R. Acad. Sci. Paris* **1976**, *282*, 887.
(4) Koval, C. A.; Segar, P. R. *J. Am. Chem. Soc.* **1989**, *111*, 2004.
(5) Koval, C. A.; Torres, R. *J. Am. Chem. Soc.* **1993**, *115*, 8368.
(6) (a) Turner, J. A.; Nozik, A. J. *Appl. Phys. Lett.* **1982**, *41*, 101. (b) Nozik, A. J.; Cooper, G.; Turner, J. A.; Parkinson, B. A. *J. Appl. Phys.* **1983**, *54*, 6463.
(7) Thévenot, D.; Buvet, R. *J. Electroanal. Chem.* **1972**, *39*, 429.
(8) Gaudiello, J. G.; Larkin, D.; Rawn, J. D.; Sosnowski, J. J.; Bancroft, E. E.; Blount, H. N. *J. Electroanal. Chem.* **1982**, *131*, 203.
(9) Raghavan, R.; Iwamoto, R. T. *J. Electroanal. Chem.* **1978**, *92*, 101.
(10) Naarova, N.; Volke, J. *Collect. Czech. Chem. Commun.* **1973**, *38*, 2670.
(11) Tokel, N. E.; Bard, A. J. *J. Am. Chem. Soc.* **1972**, *94*, 2862.
(12) Baxendale, J. H.; Fiti, M. *J. Chem. Soc., Dalton Trans.* **1972**, 1995.
(13) Seddon, E. A.; Seddon, K. R. *The Chemistry of Ruthenium*; Elsevier: Amsterdam, 1984.
(14) Henry, M. S.; Hoffman, M. Z. *J. Am. Chem. Soc.* **1977**, *99*, 5201.
(15) Mulazzani, Q. G.; Emmi, S.; Fuochi, P. G.; Hoffman, M. Z.; Venturi, M. *J. Am. Chem. Soc.* **1978**, *100*, 981.
(16) Tokel-Takvoryan, N. E.; Hemingway, R. E.; Bard, A. J. *J. Am. Chem. Soc.* **1973**, *95*, 6582.
(17) Bard, A. J.; Takvoryan, N. E. U.S. Patent 3 900 418, 1973.
(18) White, H. S.; Bard, A. J. *J. Am. Chem. Soc.* **1982**, *104*, 6891.
(19) Gleria, M.; Memming, R. *Z. Phys. Chem.* **1976,** *101***,** 171.
(20) Shaw, E. N. In *The Chemistry of Heterocyclic Compounds, Pyridine and its Derivatives*, Part 2; Klingsberg, E., Ed.; Interscience: New York, 1961.
(21) Socrates, G. *Infrared Characteristic Group Frequencies, Tables and Charts*, 2nd ed.; J. Wiley: Chichester, 1994.